JOURNAL OF MATERIALS SCIENCE. MATERIALS IN MEDICINE 4 (1993) 102–106

In vitro and *in vivo* investigation of a range of phosphate glass-reinforced polyhydroxybutyrate-based degradable composites

J. C. KNOWLES*, G. W. HASTINGS
IRC Biomedical Materials, Queen Mary and Westfield College, Mile End Road, London E1 4NS, UK

A completely degradable melt-processed composite was produced using a phosphate-based glass in the soda–lime–phosphorus pentoxide ternary phase system. *In vitro* degradation studies showed that the mass loss and mechanical property change could be closely correlated with the solubility rate of the reinforcing glass. The *in vivo* studies showed a slight inflammatory reaction, but good compatibility. With time, this inflammatory reaction disappeared and the initial reaction was interpreted as being due to a high solubility rate of the glass. The high solubility of the glass was derived not from the composition, but because the glass was in particulate form and therefore had a high surface area. This was of interest, as it showed that the polymer was highly permeable and did not encapsulate the glass as expected with a melt-processing method.

1. Introduction

Polyhydroxybutyrate (PHB) and its associated copolymers with polyhydroxyvalerate (PHV) are attracting much attention from a variety of fields [1–3]. The mechanical properties of the polymers are adequate, but the polymer has two highly exploitable properties: it is piezoelectric [4] and hydrolytically degradable [5]. The development of this material for surgical use has been undertaken because the material has also proved to be biologically acceptable in trials conducted [6]. After degradation the product breaks down to β-hydroxybutyric acid (β-HBA), a natural constituent of human blood.

Research has also been undertaken to enhance the mechanical properties [7], e.g. by the simple process of melt-forming with another phase to produce a composite, and this has proved successful. In this paper we describe the development of a composite using a phosphate-based glass as the reinforcing phase. The development of this composite was undertaken to try to develop a material with a more predictable degradation pattern, using the solubility rate of the glass filler to control the overall composite degradation.

The first part of this paper describes an *in vitro* trial that was undertaken, to determine the degradation pattern and its relationship to the glass solubility. The second stage was an *in vivo* implantation study, to determine both the biocompatibility and the degradation pattern in soft and hard tissue.

2. Materials and methods

PHB–7% PHV (M_w 580000) was obtained from Marlborough Biopolymers. A 7% incorporation of PHV enables a lower processing temperature to be used, thus ensuring less degradation during thermal processing. Glass compositions were chosen from previous work [8] and glasses with four solubility rates were used. Table I shows the mol% of each oxide required to make the particular solubility glass. The raw materials used to make the glass were mixed thoroughly and placed in a platinum crucible. This mixture was sintered at 1000 °C for 30 min. Following removal from the furnace, the glass was poured on to a steel table to cool. Subsequently, the glass was ground in a vibratory mill to obtain a powder of particle size $< 14\,\mu m$. To produce a composite, the glass and polymer (both in powder form) were automixed at a glass addition up to 40 wt % and injection moulded to form standard tensile test pieces.

2.1. *In vitro* studies

To produce specimens for the *in vitro* studies, composites with a glass filler addition of 40 wt % were produced for injection moulding to form standard dumbbell-shaped tensile test pieces. These injection moulded specimens for *in vitro* degradation were placed in phosphate-buffered saline (PBS) at pH 7.4. This was maintained at 37 °C. At the appropriate time

* Author to whom all correspondence should be addressed.

0957–4530

specimens were removed from the solution for testing. To identify the four composites they are referred to by the solubility rate of the glass filler used, i.e. 0.5, 0.25, 0.17 and 0.065 (Table I).

All mechanical testing of specimens was performed on an ESH hydraulic testing machine. The specimens were tested at a displacement of 5 mm min^{-1} (strain rate 5%) until failure and the subsequent load–extension outputs were recorded on a flat-bed plotter. From this graph the slope of the linear part of the curve was used to calculate the Young's modulus (E). The ultimate tensile strength (UTS) and percentage elongation at failure (%e) were also determined. To determine the wet and dry weights, the samples were, at the appropriate time, removed from solution and the surface was wiped clean of excess moisture. Following weighing, the samples were dried for 24 h at 50 °C and then weighed again. The weight was plotted as a percentage of the initial weight using

$$\% \text{ wet weight} = \frac{\text{wet weight at time } t - \text{initial dry weight}}{\text{initial dry weight}} \times 100$$

$$\% \text{ dry weight} = \frac{\text{dry weight at time } t - \text{initial dry weight}}{\text{initial dry weight}} \times 100$$

2.2. *In vivo* studies

The *in vivo* study was in two parts, a subcutaneous-type (SC) implant and a non-load-bearing femoral (NL) implant. Both the SC and the NL implants were machined from the central section of tensile test pieces produced by injection moulding. Three solubility rate implants were produced for both the SC and the NL: a rapidly dissolving implant using glass type 0.5, a medium-rate dissolving implant using glass type 0.25 and a slowly dissolving implant using glass type 0.065.

For the SC implant the composite was machined to produce an implant of dimensions 10 mm × 8 mm × 2 mm. Using 10-week-old male Wistar rats and under halothane anaesthesia, an incision was made in the skin overlying the muscles of the hindlimb. The implant was sterilized with alcohol and inserted into the wound. Closure was by skin clips.

For the NL implants, 16-week-old male Wistar rats were used. Again, using halothane anaesthesia, an incision was made through the skin and the muscles overlying the femur were retracted to expose the midshaft. A hole 2 mm in diameter was made in the lateral wall of the femur and a rivet-shaped implant 2 mm in diameter was inserted. Closure was performed subcutaneously with Vicryl 4/0 sutures and then the skin was closed with skin clips.

2.3. Specimen processing: SC implant

For the SC implants, at 2, 4, 8 and 12 weeks, the appropriate rats were killed by exsanguination under anaesthesia and the blood collected with a heparin anticoagulant. The blood was centrifuged at 1500 r.p.m. for 5 min to obtain the plasma. Three cuvettes were used for each sample: reagent blank, control and sample. To each of these tubes 3.0 ml β-HBA reagent and 0.05 ml β-hydroxybutyrate (β-HBDH) was added and warmed to 37 °C. To the blank tube 0.05 ml deionized water was added, 0.05 ml β-HBA calibrator to the calibrator cuvette (containing 50 mg dl^{-1} β-HBA) and finally 0.05 ml plasma to the sample cuvette. The cuvettes were warmed at 37 °C for 10 min and then the absorbance at 340 nm was measured.

TABLE I Composition (mol %) of oxides to form the required solubility glasses

Oxide	Solubility rate (mg cm^{-2} h^{-1})			
	0.065	0.17	0.25	0.5
Soda	20.00	34.15	27.8	34
Lime	25.7	22.84	29.8	27
Phosphorus pentoxide	54.3	43.00	42 5	39

2.4. Determination of β-HBA concentration

$$sA = A(\text{sample}) - A(\text{blank})$$

$$\text{serum β-HBA (mg dl}^{-1}) = sA \times 104$$

To convert to SI units (mmol l^{-1}), the β-HBA concentration (mg dl^{-1}) is multiplied by 0.096. A kit obtainable from Sigma Chemical Co. (procedure no. 310-UV) was used for determination of the PHB levels in the plasma. Utilizing the reaction

$$\text{β-hydroxybutyrate} + \text{NAD} \rightarrow \text{acetoacetate} + \text{NADH}$$

A catalyst β-HBDH catalyses the oxidation of β-HBA to acetoacetate. During this reaction an equimolar amount of nicotinamide–adenine dinucleotide (NAD) is reduced to NADH. At wavelength 340 nm NADH absorbs light, hence the increase in absorbance in light is directly proportional to the β-HBDH concentration in the serum sample.

For the implant processing, the skin overlying the implant, and the implant and surrounding tissue were removed. The sample was placed in buffered formalin and processed using standard soft-tissue techniques. The sections were stained using haemotoxylin and eosin (H & E).

2.5. Specimen processing: NL implants

The NL implants were also processed by similar methods, but the bone specimens were decalcified before sectioning. H & E staining was again used.

3. Results

3.1. *In vitro* studies

Figs 1 and 2 show the wet and dry weight loss with time. The curves show a very characteristic initial

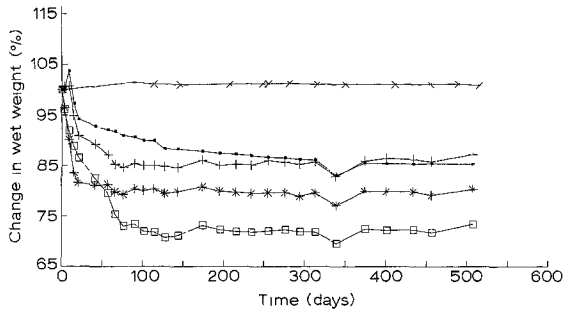

Figure 1 In vitro (PBS, pH 7.4, 37 °C) wet weight change with time for the different composites. (×) unfilled, (●) 0.065, (+) 0 17, (∗) 0.25 and (□) 0.5

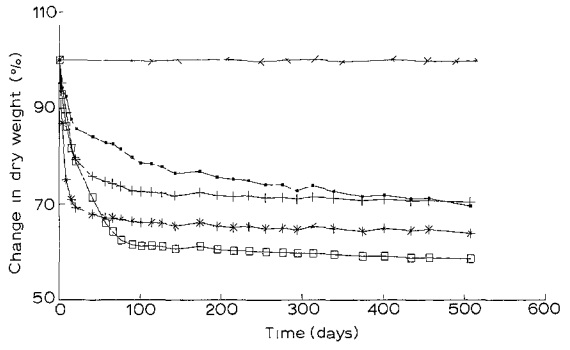

Figure 2 In vitro (PBS, pH 7.4, 37 °C) dry weight change with time for the different composites (×) unfilled, (●) 0.065, (+) 0.17, (∗) 0 25 and (□) 0.5.

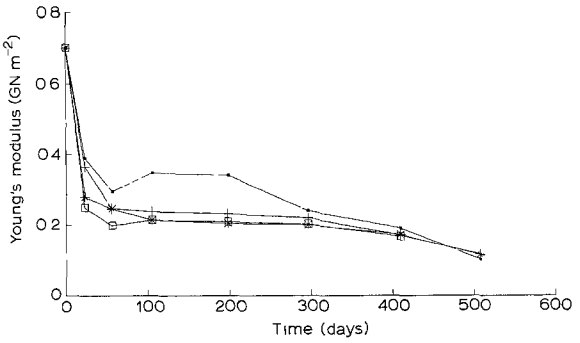

Figure 3 In vitro (PBS, pH 7.4, 37 °C) Young's modulus change with time for the different composites: (●) 0.065, (+) 0.17, (∗) 0.25 and (□) 0.5.

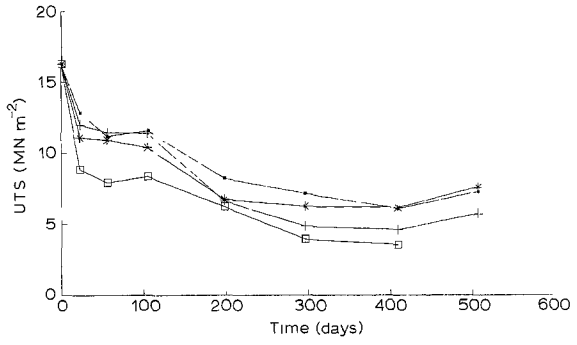

Figure 4 In vitro (PBS, pH 7.4, 37 °C) UTS change with time for the different composites: (●) 0.065, (+) 0.17, (∗) 0 25 and (□) 0.5

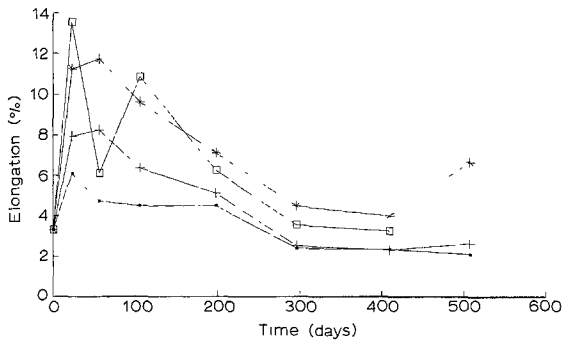

Figure 5 In vitro (PBS, pH 7.4, 37 °C) wet weight change with time for the different composites: (●) 0 065, (+) 0 17, (∗) 0.25 and (□) 0.5

weight loss with time regardless of the filler solubility. This first stage is followed by a state of equilibrium. The figures clearly show a relationship between the filler solubility and the degradation rate. For Fig. 1 the small dip at about 350 days may be accounted for as being due to a measurement artefact.

For the change in stiffness and UTS with time, shown in Figs 3 and 4, respectively, the specimens exhibited a similar trend to that seen for the weight loss. Of note with the stiffness changes is that the samples continued to decrease in stiffness, unlike the weight loss curves. The %e with time showed a slightly different pattern (Fig. 5). All samples showed an initial sharp rise in value, followed by a steady decline with time of exposure to solution.

3.2. *In vivo* studies

3.2.1. SC implant

Fig. 6 shows the change in the HBA level in the blood with time. With increasing length of time of implantation there was an increase in the level of HBA in the blood, but the changes were not significant. With the statistical variation found between implant types, no relationship could be found between the filler solubility and the blood HBA levels.

For the histological results, a clear change in the level of cellular activity with time could be seen. At 4 weeks (Fig. 7) there were many fibroblasts present surrounding the implant, and these fibroblasts were laying down collagen to encapsulate the implant. There were two points of interest with the SC implants: the implants showed the highest cellular density at some distance from the implant surface, and the level of reaction between the skin and the muscle side of the implant was different.

At 8 weeks the cellular activity was considerably reduced (Fig. 8). The fibrous capsule surrounding the implant became significantly reduced and was only of the order of a few cells thick. The collagen also became highly ordered (orientated).

At 12 weeks (Fig. 9) the cellular activity around the implant had subsided even further. The capsule had become thinner than that seen at 8 weeks.

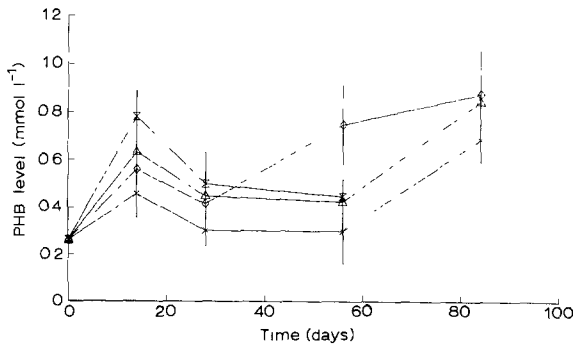

Figure 6 In vivo blood level change with time for the different composites: (×) control, (◇) 0.065, (△) 0.25 and (⧖) 0.5.

Figure 7 Histological section of SC/0.065/4 (H & E) (×125).

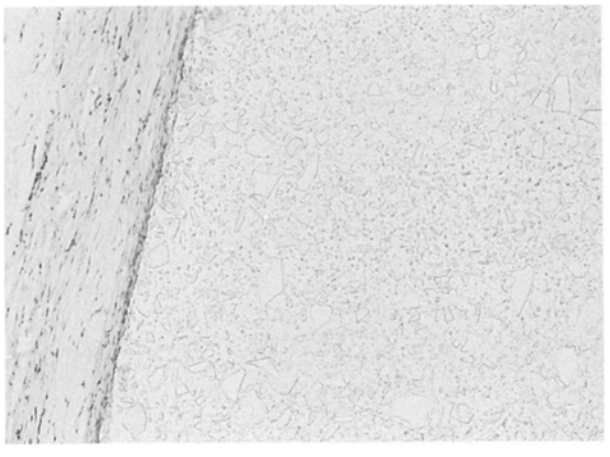

Figure 8 Histological section of SC/0.065/8 (H & E) (×125).

3.2.2. NL implant

At 4 weeks some inflammatory cells at the bone–implant interface could be seen on the slowly degrading implant and the cells found at the interface formed a definite boundary. The majority of the cells were fibroblasts and the implant–tissue boundary could be seen to be very intimate, with good cellular adhesion to the surface of the implant with cell growth into the voids created by the glass that had been removed from the composite surface. This same close

Figure 9 Histological section of SC/0.065/12 (H & E) (×125).

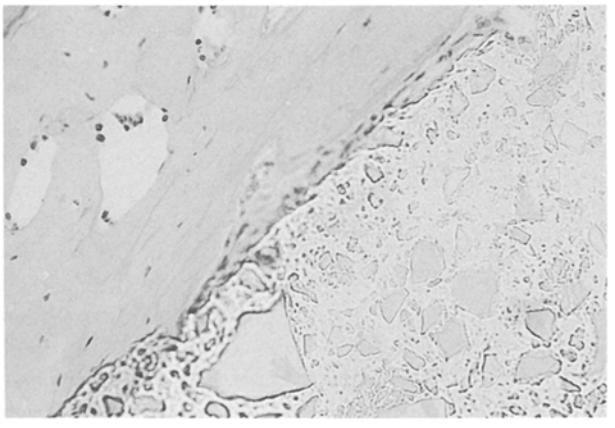

Figure 10 Decalcified section of NL/0.065/8 (H & E) (×312.5).

interface could be found for the other solubility composites.

Eight weeks postoperatively the tissue reaction of the slowly soluble composite had changed considerably (Fig. 10). The surrounding bone could be seen to be growing close to the surface of the NL implant. A thin layer of fibroblasts at the implant interface could be seen at the bone–implant interface.

At 12 weeks the fibroblasts had disappeared and the bone could be seen to be growing directly on the implant surface (Fig. 11). The implant surface was also starting to show signs of degradation, indicated by the increase in surface roughness.

4. Discussion

For the *in vitro* studies the solubility rate of the glass filler could be seen to be controlling the change in physical properties. The wet and dry weight losses may be attributed to the dissolution of the glass from the composites. Consideration of the mechanical properties shows that they are closely related to the weight loss curves. For E and the UTS the initial rapid drop in strength is due to the stiffer reinforcing glass phase dissolving out. For the %e the same applies. The relative proportion of polymer (with a higher %e) in the composite is increasing, hence the increase in %e with time.

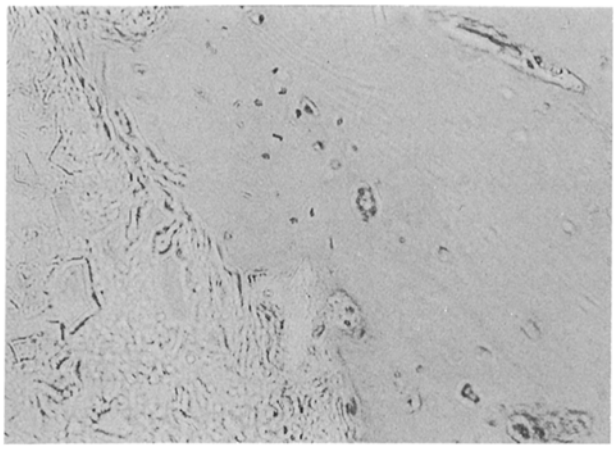

Figure 11 Decalcified section of NL/0.065/12 (H & E) (×312.5).

The *in vivo* work is clearly related to the *in vitro* work. The blood levels of HBA are only slowly increasing, as the polymer, although it will have started to degrade, will not be releasing significant amounts of HBA systemically.

For the histological examination of the SC implants, an initial high cellular density was initiated by ion release from the soluble glass. Autian [9] suggested that biocompatibility may be quantitatively assessed by the thickness of the fibrous tissue capsule around an implant. This work has highlighted two reasons for not considering his method: first, the cellular density is not highest at the implant surface and, secondly, the cellular reaction after 8 weeks is slow, i.e. there has been a very large change in the mode of tissue reaction.

Thus, the reaction needs to be assessed in terms of both the cellular density and the amount of collagen. For the NL implants the initial reaction seen correlates with those seen for the SC implants. The initial fast reaction quickly subsides to allow normal cellular activity to occur. With the NL implants bone growth adjacent to the implant surface may be clearly seen, indicating good compatibility.

5. Conclusion

A comparison of this new composite with similar materials such as polyglycolic acid (PGA) and poly(L-Lactide) (PLA) shows a considerable difference in the degradation pattern, both *in vitro* [10, 11] and *in vivo* [12, 13]. Recent *in vivo* trials [14] on PGA showed that the material produced a low initial fibroblastic response that increased with time as the implant degraded. The implants of PGA and PLA also degraded quickly, perhaps too quickly for potential orthopaedic use. The PHB/glass composite, however, elicited an initial high cellular reaction, which subsided to give little or no inflammation. Also, the overall degradation profile was much longer than that found for the PGA and PLA.

Of further interest with the PHB/glass composite is the concept of enhanced bone formation. The use of materials such as hydroxyapatite has shown rapid new bone formation [15, 16] due to the close match of the mineral structure of hydroxyapatite and the inorganic phase of bone. The PHB/glass composite may give enhanced bone formation from a more chemical route. The dissolution of the glass will release Ca^{2+} and P^{5+} ions into the surrounding tissue, giving the bone-forming osteoblasts the necessary precursors for laying down hard tissue.

References

1. E. FUKADA and Y ANDO, *Int. J. Biol. Macromol* **8** (1986) 361
2. S J HOLLAND, M YASIN and B J. TIGHE, *Biomaterials* **11** (1990) 206
3. Y. DOI, Y. KANESAWA, M KUNIOKA and T SAITO, *Macromolecules* **23** (1990) 26.
4. J C KNOWLES, F A. MAHMUD and G. W HASTINGS, *Clin. Mater.* **8** (1991) 155.
5. J C. KNOWLES and G W. HASTINGS, *Biomaterials* **12** (1991) 210.
6. N. D MILLER and D F WILLIAMS, *ibid.* **8** (1987) 129.
7. K. E TANNER, C. DOYLE and W BONFIELD, in "Clinical Implant Materials", edited by G. Heimke, U. Soltesz and A J. C. Lee (Elsevier Science, Amsterdam, 1990).
8. J BURNIE, PhD thesis, University of Strathclyde (1982).
9. J AUTIAN, *Artif. Organs* **1** (1977).
10. S VAINIONPAA, J. KILPIKARI, J LAIHO, P. HELEVIRTA, P ROKKANEN and P TORMALA, *Biomaterials* **8** (1987) 46.
11. J W LEENSLAG, A. J PENNINGS, R. R. M BOS, F R ROZEMA and G BOERING, *ibid.* **8** (1987) 311.
12. J. VASENIUS, S. VAINIONPAA, K. VIHTONEN, A MAKELA, M. MERO, P. ROKKANEN and P. TORMALA, *ibid.* **11** (1989) 501.
13. P TORMALA, J. VASENIUS, S VAINIONPAA, J LAIHO, T. POHJONEN and P ROKKANEN, *J. Biomed. Mater. Res.* **25** (1991) 1.
14. R R M BOS, F R ROZEMA, G BOERING, A. J. NIJENHUIS, A J. PENNINGS, A B VERWEY, P. NIEUWENHUIS and H W. B. JANSEN, *Biomaterials* **12** (1991) 32.
15. H OONISHI, S KUSHITANI, M. AONO, Y UKON, M. YAMAMOTO, H ISHIMARU and E. TSUJI, *J. Bone Joint Surg.* **71B** (1989) 213
16. A. M. GATTI, D. ZAFFE and G. P. POLI, *Biomaterials* **11** (1990) 513.

Received 15 October 1991
and accepted 19 February 1992